ELSEVIER

Pharmacological Research 55 (2007) 49–56

Pharmacological research

www.elsevier.com/locate/yphrs

Poly(ADPR)polymerase-1 signalling of the DNA damage induced by DNA topoisomerase I poison in D54^{p53wt} and U251^{p53mut} glioblastoma cell lines

Gabriella Cimmino [a], Stefano Pepe [b], Gianluca Laus [b], Maria Chianese [b], Daniela Prece [a], Romina Penitente [a], Piera Quesada [a,*]

[a] *Department of Functional and Structural Biology, University "Federico II", Naples, Italy*
[b] *Department of Molecular and Clinical Endocrinology and Oncology, University "Federico II", Naples, Italy*

Accepted 16 October 2006

Abstract

Glioblastomas are widely characterised by the mutation of the p53 gene and p53 disruption sensitizes glioblastoma cells to DNA topoisomerase I (TOPO I) inhibitor-mediated apoptosis.

We investigated the effects of combined treatments with the DNA topoisomerase I inhibitor Topotecan and the poly(ADPR)polymerase-1 inhibitor NU1025 in D54^{p53wt} and U251^{p53mut} glioblastoma cell lines. Analysis of cell growth and cell cycle kinetics showed a synergistic anti-proliferative effect of 10 nM TPT and 10 μM NU1025 and a G_2/M block of the cell cycle.

We also evaluated, the influence of TPT+/−NU1025 treatment on PARP-1 and p53 activity. We got evidences of a TPT-dependent increase of PARP-1 auto-modification level in both the cells. Moreover, in the D54^{p53wt} cells we found that in co-treatments NU1025 incremented the TPT-dependent stimulation of p53 transcriptional activity and increased the p21 nuclear amount. Conversely, in U251^{p53mut} cells we found that NU1025 incremented the TPT-dependent apoptosis characterised by PARP-1 proteolysis.

Our findings suggest that the modulation of PARP-1 can be considered a strategy in the potentiation of the chemotherapeutic action of TOPO I poisons in glioblastoma cells apart from their p53 status.

Keywords: Glioblastoma cells; Topotecan; NU1025; PARP-1; TOPO I; p53; p21

1. Introduction

Despite research efforts the overall survival of patients affected by glioblastoma tumors is still scarce; chemotherapeutic treatment has been hampered by the resistance of these tumor cells to available agents [1].

Glioblastomas are widely characterised by the mutation of the p53 gene [2] and it has been reported that p53 disruption sensitizes glioblastoma cells to DNA topoisomerase I (TOPO I) inhibitor-mediated apoptosis [3].

TOPO I plays its role relieving the torsional stress generated during replication, recombination and transcription. During the relaxation reaction, a covalent intermediate between TOPO I and 3′-single-stranded DNA breaks is formed and this *cleavable complex* become stabilized in the presence of TOPO I inhibitors. According to the "fork collision model", irreversible damage to the DNA occurs when a DNA replication fork encounters such stabilized *cleavable complexes*, resulting in the formation of lethal DNA double strand breaks [4].

Preclinical and clinical data demonstrated that the TOPO I inhibitor topotecan (TPT) is able to penetrate the blood–brain barrier and demonstrated considerable activity against a panel of xenografts derived from human glioblastomas, ependymomas, and medulloblastomas [5,6]. TPT is under clinical investigation in the treatment of human CNS tumors, but phase II trials of TPT for adults with newly diagnosed or recurrent malignant glioma showed only a modest activity [7]. In this regard, several data demonstrate that inhibition of poly(ADPR)polymerase-1 (PARP-1) enzyme potentiates the action of TOPO I inhibitors in a panel of human tumor cell lines [8].

Poly(ADP-ribosyl)ation is a post-translational protein modification that occurs immediately after exposure of cells to DNA damaging agents [9]. *In vivo*, 90% of ADP-ribose polymers

* Corresponding author at: Department of Structural and Functional Biology, Via Cinthia Monte S. Angelo, 80126 Napoli, Italy. Tel.: +39 081 679 165; fax: +39 081 679 233.
E-mail address: quesada@unina.it (P. Quesada).

1043-6618/$ – see front matter © 2006 Elsevier Ltd. All rights reserved.
doi:10.1016/j.phrs.2006.10.005

(PAR) deriving by the use of β-NAD^+ substrate, are attached to the auto-modification domain of PARP-1, the main enzyme catalysing this reaction [10].

Moreover, the PAR chains (up to 200 residues long) linked to PARP-1 are able to not covalently interact with several target proteins containing a "polymer-binding motif" [11].

PARP-1 has been found to covalently poly(ADP-ribosyl)ate a number of nuclear components (hetero-modification) either structural and functional proteins [9,10]. Several observations support a relationship between p53 and PARP-1: both covalent [12] and non-covalent interactions between p53 and PAR modulate the binding of p53 to its consensus sequence [13]. Ferro and Olivera [14] first demonstrated that TOPO I can be poly(ADP-ribosyl)ated.

Moreover, PARP-1 is subject to cleavage by caspases into two fragments of 89 kDa and of 24 kDa, thereby avoiding futile cycling of PAR that would otherwise deplete the cell of β-NAD^+ required for the onset of apoptosis [15].

Data deriving from *parp-1*$^{-/-}$ or *parp-2*$^{-/-}$ mice or by the use of chemical inhibitors clearly indicate that abrogation of enzyme activity increases cell susceptibility to DNA damaging agents and enhances the efficacy of chemo- and radiotherapy. Indeed, the restoration of the apoptotic program in neoplastic cells is considered a new frontier in the treatment of cancers. Based on the original benzamide structure template, a wide panel of PARPs inhibitors have been synthesized, that exhibit enhanced potency and specificity [16]. Among them 8-hydroxy-2-methylquinazolinone-4-one (NU1025) showed an additive effect on TOPO I cytotoxicity in several tumor cells [8,17].

With the aim to explore a possible way to increase the efficacy of TPT in glioblastoma cells, we investigated the effects of TPT and NU1025 on *in vitro* models of human glioblastoma cell line, $D54^{p53wt}$ and $U251^{p53mut}$ (codon 273). Both cell lines were treated with different dosages of TPT in combination with NU1025. Cell growth inhibition, cell cycle kinetics and the degree of apoptosis showed that NU1025 was able to enhance the cytotoxic effects of TPT in a synergistic manner. Moreover, we investigated the effects of TPT and NU1025 on PARP-1 enzymatic activity and p53 transcriptional activity. Our findings revealed that both proteins are involved in the signalling of the DNA damage deriving from TOPO I inhibition.

2. Materials and methods

2.1. Cell culture and reagents

The human glioblastoma cell lines D54 and U251 (gift from Dr. D. Raben) were maintained in Dulbecco's modified Eagle's medium (DMEM) and Ham's nutrient mixture F-12 (Ham's) 1:1 (Cambrex), containing 10% (v/v) heat-inactivated foetal bovine serum (FBS, Bio Whittaker), 100 U/ml penicillin, 100 μg/ml streptomycin, 5 mM L-glutamine (Cambrex) and incubated at 37 °C in a humidified atmosphere, *plus* 5% CO_2.

Topotecan (TPT) was from Glaxo Smith-Kline and 8-hydroxy-2 methylquinazolinone-4-one (NU1025) from Alexis Biochemicals. [^{3}H]NAD^+ nicotinamide (Nicotinamide 3,5,8[^{3}H] adenine dinucleotide 250 mCi/mmol) was from Amersham International. Propidium iodide (PI) and RNAse were from Sigma Chemicals Co. Anti-PAR mouse monoclonal antibody (H-10), anti-PARP-1 mouse monoclonal antibody (F1–23) and anti-polyclonal 89 kDa fragment of PARP-1 (214/215) were from Alexis Biochemicals. Anti-p53 mouse monoclonal antibody (DO-1), anti-p21 mouse monoclonal antibody (C-19) and anti-α-actinin mouse monoclonal antibody (H-2) were from Santa-Cruz Biotechnology Inc. Anti-DNA topoisomerase I human antibody (Scl-70) and protein A–peroxidase were from Topogen. Goat anti-mouse and goat anti-rabbit IgG HRP-conjugate was from Sigma.

2.2. Cell growth inhibition

D54 and U251 cells were seeded in 96-multiwell plates at 2.5×10^3 cells. After 24 h, cell cultures were treated with different concentrations of TPT and NU1025 and cell growth inhibition was assessed at different time points (24, 48, 72 and 96 h) using the 3-[4,5-dimethylthiazol-2-yl]-2,5-diphenyltetrazolium bromide (MTT) assay. All the experiments were performed in triplicate.

Drug combination studies were based on concentration–effect curves generated as a plot of the fraction of affected/killed cells versus combination index, performed by the *Calcusyn* software program [18]. The general equation for the classic isobologram is given by

$$\mathrm{CI} = \frac{(D)_1 + (D)_2}{(D_x)_1 + (D_x)_2}$$

where $(D)_1$ and $(D)_2$ in the numerators are the doses of drugs 1 and 2 alone that gives x% inhibition, whereas $(D_x)_1$ and $(D_x)_2$ in the denominators are the doses for drug 1 drug 2 in combination that also inhibited x%. CI < 1, CI = 1 and CI > 1 indicate synergism, additive effect, and antagonism, respectively.

2.3. Cytofluorimetric analysis

Control and treated cells were detached by enzymatic treatment (Trypsin/EDTA 0.02%), washed in PBS $^{w/o\ Ca++/Mg++}$ pooled with floating cells and recovered by centrifugation at 1200 rpm for 15 min at 4 °C. Cells were fixed in 70% ethanol and stored at −20 °C until analysis.

After a washing in PBS $^{w/o\ Ca++/Mg++}$, cells were stained in 2 ml of PI staining solution (50 μg/ml of PI, 1 mg/ml of RNAse in PBS $^{w/o\ Ca++/Mg++}$, pH 7.4) overnight at 4 °C and DNA-flow cytometry was performed in duplicate by a FACScan flow cytometer (Becton Dickinson) coupled with a CICERO work station (Cytomation). Cell cycle analysis was performed by the ModFit LT software (Verity Software House Inc.). FL2 *area* versus FL2 *width* gating was done to exclude doublets from the G_2M region. For each sample 15,000 events were stored in list mode file.

Terminal deoxyribonucleotide tranferase-mediated dUTP-X nick-end labelling (TUNEL) assay was performed by using the

"*In situ* Cell Death Detection Kit" (Roche Applied Science) according to the manufacturer's instructions. After 60 min at 37 °C, samples were diluted in 0.5 ml of PBS and analyzed by flow-cytometry. For each samples, 5000 events have been analysed. Incorporated FITC-dUTP signals were registered in the FL1 channel (log scale) and analyzed by the Cyclops SUMMIT software.

2.4. Isolation of nuclear and post-nuclear fractions

Isolation of sub-cellular fractions was carried out in cells suspended in a buffer containing 0.32 M Sucrose, 10 mM Tris–HCl pH 7.8, 2 mM $MgCl_2$, 5 mM β-mercaptoethanol, 2 mM PMSF, 1% (v/v) Triton X-100 and the protease inhibitors cocktail solution (Roche Diagnostics). After five strokes with the Dounce homogeniser and 15 min of incubation on ice, cellular suspensions were centrifuged at 800 × *g* for 10 min at 4 °C and the nuclear fractions recovered in the pellet. The supernatant represents the post-nuclear fraction.

Protein extract from cells and nuclear fractions were obtained in 40 mM Tris–HCl pH 7.8, containing 0.6 mM EDTA, 1 mM β-mercaptoethanol, 30 mM $MgCl_2$, 0.05% Triton X-100, 20% glycerol and the protease inhibitors cocktail solution, 30 min 0 °C. Protein concentration was determined using the Bradford protein assay reagent (BioRad) with bovine serum albumin as a standard.

2.5. Poly(ADPR) polymerase assay

PARP-1 activity assay was performed in permeabilised cells according to the protocol reported by Virag L. in the PARP link homepage (http://parplink.u-strasbg.fr/index.html). Briefly, the cells in a reaction mixture composed of 50 mM HEPES (pH 7.5), 28 mM KCl, 28 mM NaCl, 2 mM $MgCl_2$, 0.01% (v/v) digitonin, 0.125 μM NAD^+ and 0.5 μCi/ml [^{3}H]NAD^+ where incubated 10 min at 37 °C. The radioactivity recovered in the TCA-insoluble material suspended in 500 μl of 2% SDS/0.1 M NaOH and incubated 3 h at 37 °C, was counted in a Beckman LS8100 liquid scintillation spectrometer and expressed as nmol of [^{3}H]PAR/10^6 cells. The data represent means of three experiments done in duplicate ±S.E.

2.6. Western blotting analysis

Protein extracts (100 μg) were separated by SDS-PAGE (5–15% gradient gels) and transferred onto a PVDF membrane using an electro-blotting apparatus. The membrane was incubated with 3% (w/v) non-fat milk in 20 mM Tris–HCl pH 8, 150 mM NaCl and 0.5% (v/v) Tween 20 (TBST) with antibodies anti-PARP-1 (diluted 1:5000), anti-89 kDa fragment of PARP-1 (diluted 1:200), anti-p53 (diluted 1:2000), anti-p21 (diluted 1:500), anti-TOPO I (diluted 1:5000), anti-α-actinin (diluted 1:200). As secondary antibodies goat-anti-mouse, or goat-anti-rabbit IgG HRP-conjugate (diluted 1:2000–1:4000) or protein A–peroxidase HRP-conjugate (diluted 1:20,000) in 3% (w/v) non-fat milk in TBST were used. Peroxidase activity was detected using the Luminol reagent (SantaCruz) and quantified using the Immuno-Star Chemioluminescent detection system (BioRad).

3. Results

In both cell lines, a dose-dependent growth inhibition was observed following treatment with 10–1000 nM TPT for 24, 48, and 72 h. We found that 10 nM TPT induced a 50% and 70% growth inhibition after 72 h treatment in D54 and U251 cells, respectively. NU1025 had not effect *per se* on cell growth up to 150 μM (data not shown).

PARPs inhibitory efficiency of NU1025 was defined in comparison with 3-ABA, by the previously reported enzymatic activity assay [19], in the presence of 200 μM [^{14}C]NAD^+. The addition of 10 μM NU1025 or 1 mM 3-ABA caused a 98% inhibition of PARP specific activity (data not shown).

The effects of TPT and NU1025 combined treatments on both cell lines were evaluated by the MTT assay using five different TPT/NU1025 molar ratios (1:10, 1:100, 1:1000, 1:10,000 and 1:100,000) and the resulting data were elaborated according to Chou and Talalay by the *Calcusyn* software [18]. As shown in Fig. 1, the concentration–effect curves generated as a plot of the

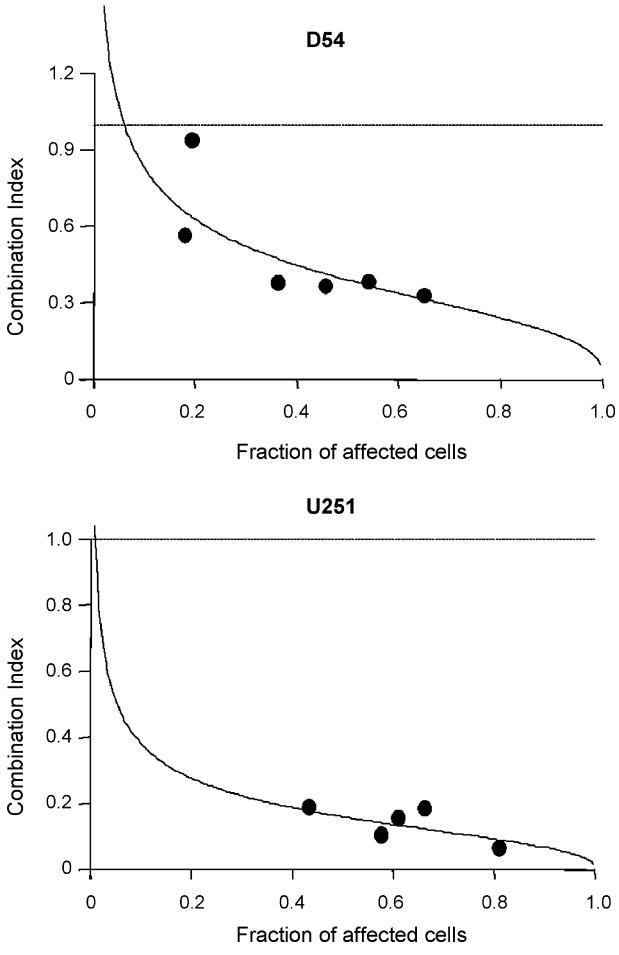

Fig. 1. Isobologram analysis of D54 and U251 cells after TPT and NU1025 48 h combined treatment at molar ratio 1:1000. Combinations were considered synergistic when CIs were <1. The figure shows the results of a representative experiment carried out at least three times for each cell line.

Table 1
Analysis of the synergistic effect of TPT and NU1025

Cell line	Combination ratio (TPT:NU1025)	CI50	DRI50	Interpretation
D54	1:1000	0.113	TPT 8.87	Strong synergism
U251	1:1000	0.389	TPT 2.57	Synergism

fraction of affected/killed cells versus combination index (see Section 2) demonstrated a CI < 1 in both cell lines when the two drugs were used at the molar ratio of 1:1000. Table 1 reports a $CI_{50} = 0.113$ for D54 cells and $CI_{50} = 0.389$ for U251, respectively, showing a strong synergistic anti-proliferative effect. In addition, the *Calcusyn* software allowed to calculate a dose reduction index (DRI_{50}), which represents the magnitude of reduction of the dose that inhibits cell growth by 50% in a combination setting, as compared to each drug alone. In our experimental conditions, the DRI_{50} of TPT was 8.87 in $D54^{p53wt}$ and 2.57 in $U251^{p53mut}$. Notably, the synergism of PARP-1 inhibitor was more relevant in $D54^{p53wt}$ than in $U251^{p53mut}$, that is *per se* less sensitive to the TOPO I inhibitor.

The degree of cell cycle perturbation in D54 and U251 cells at different times of treatments is shown in Fig. 2. Cell cycle kinetics of D54 cells was unaffected by 10 μM NU1025; 10 nM TPT induced a modest G_2M cell accumulation at 48 h, while 10 nM TPT + 10 μM NU1025 induced a more sustained G_2M arrest.

Also U251 cell cycle was unaffected by 10 μM NU1025 alone, while 10 nM TPT induced a strong G_2M cells accumulation at 48 h, which persisted at 72 h. Such an effect was further enhanced by the addiction of 10 μM NU1025, resulting in the almost total block in late S/G_2M phases of the cell cycle.

The involvement of PARP in the signalling of DNA damage deriving from TOPO I inhibition was confirmed by monitoring PARP activity in control and TPT-treated D54 and U251 cells.

The enzymatic assay showed a slightly higher activity in D54 than in U251 ($0.66 - 0.48$ pmol of $[^3H]PAR \times 10^6$ cells).

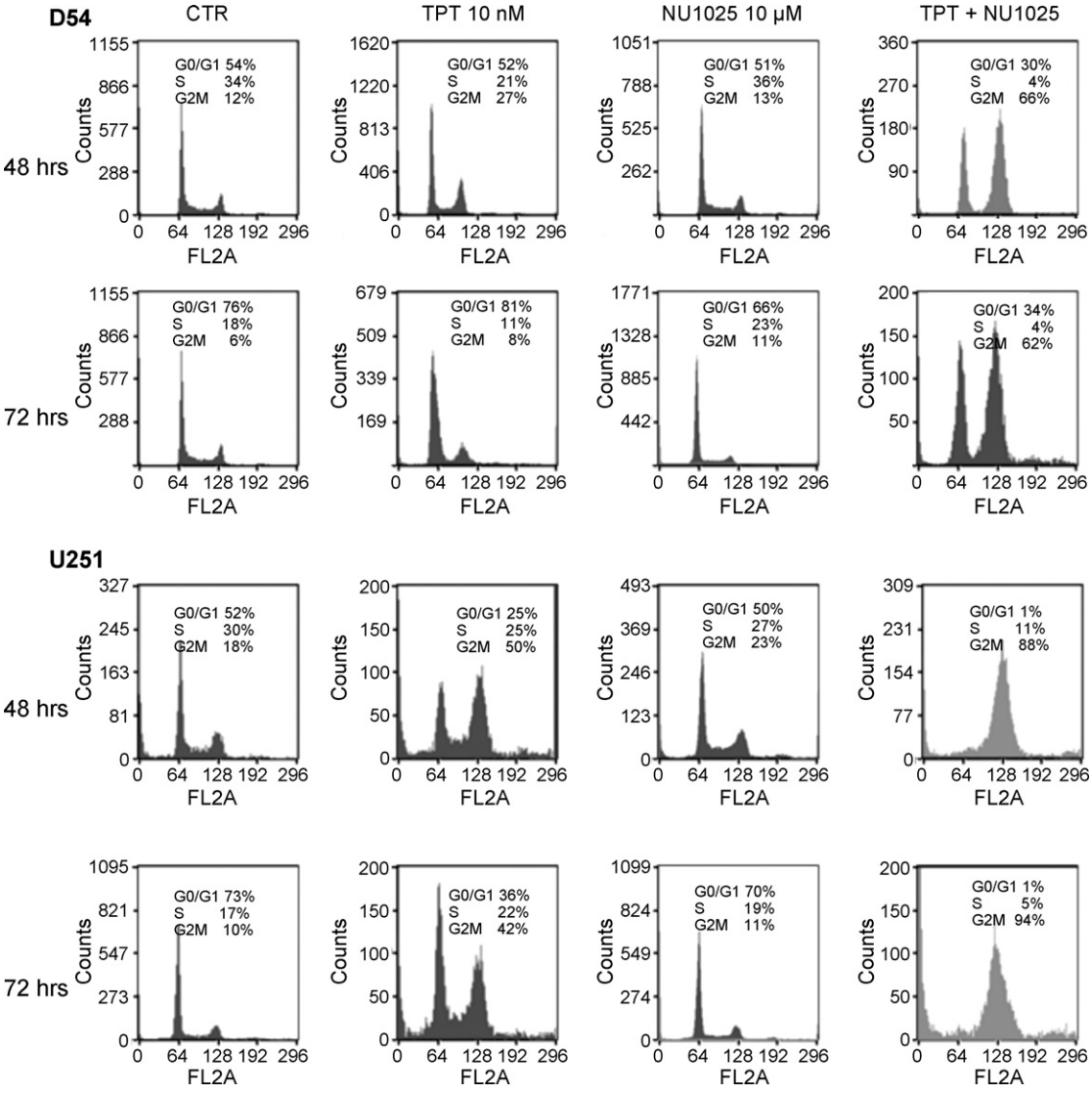

Fig. 2. Flow cytometric analysis of cell cycle perturbation induced by 10 nM TPT ± 10 μM NU1025. The percentage of D54 and U251 cells in the different phases of cell cycle are indicated. Data refer to one of three experiments giving similar results.

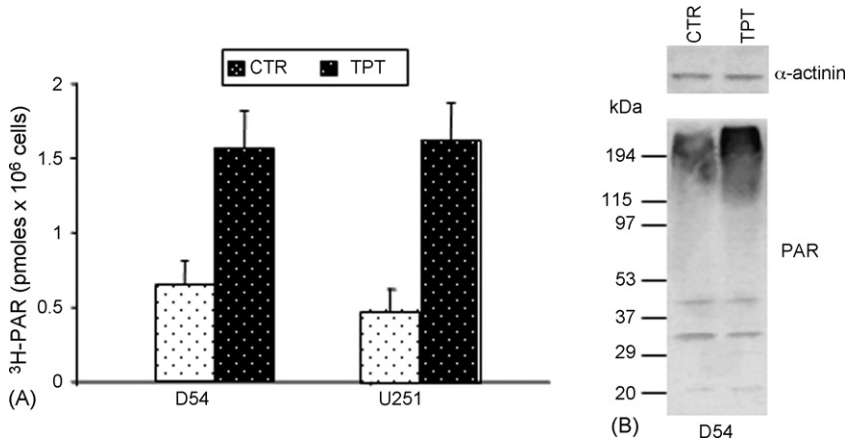

Fig. 3. (A) [^{3}H]PAR amount in control and 24 h 10 nM TPT-treated U251 and D54 cells. The bars indicate the S.E. calculated for three different experiments done in duplicate: $P = 0.004$. (B) Western blotting analysis of D54 control and 24 h 10 nM TPT-treated cells with the anti-PAR and the anti-α-actinin antibody used as loading control.

Furthermore, we found that 10 nM TPT induced a two-fold increase of PARP activity 24 h after treatment in both cell lines (Fig. 3A).

This result was confirmed by Western blotting analysis of D54 cells with an anti-PAR antibody (Fig. 3B). The broad immunoreactive band above the migration region of PARP-1 (116 kDa) identified the auto-modified form of PARP-1 enzyme and was much more intense in the sample from TPT-treated than from control cell. A similar result was obtained for U251 cells (data not shown).

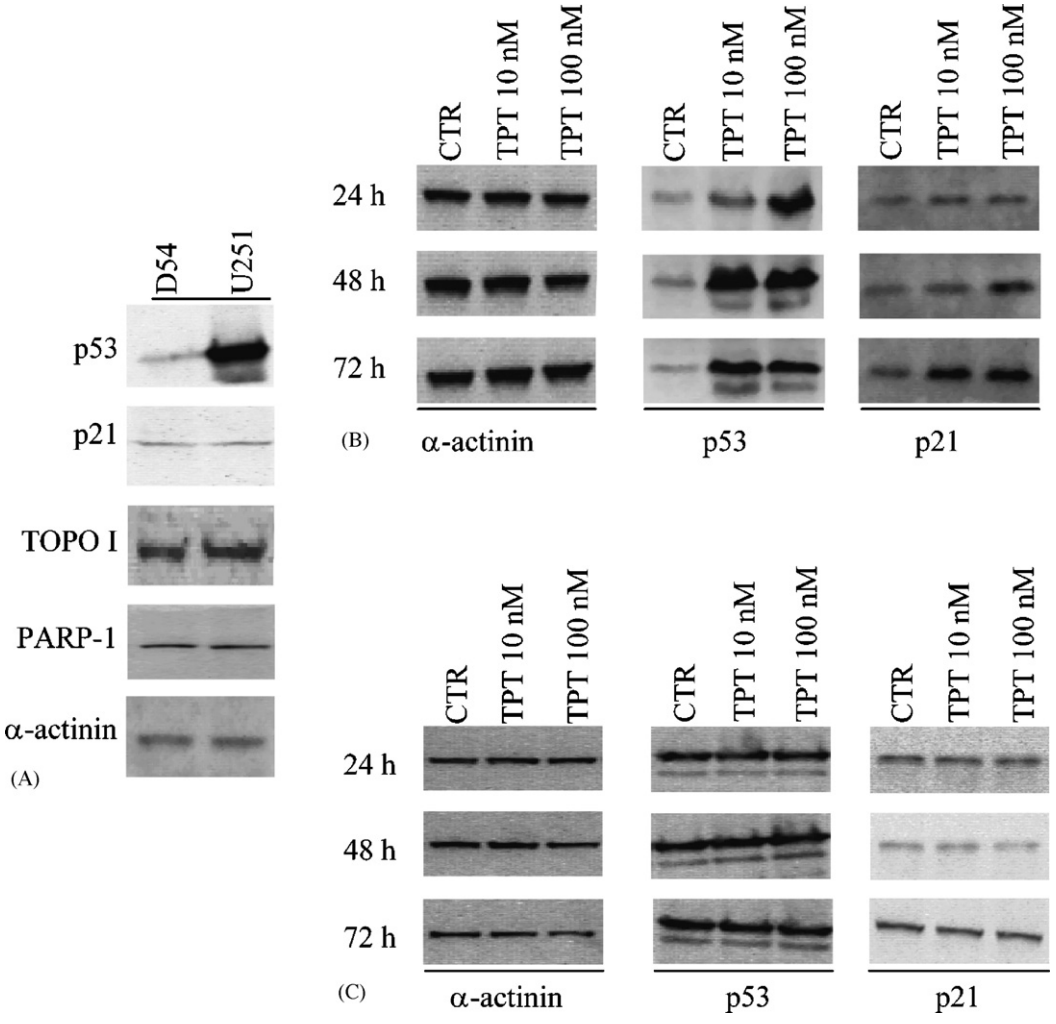

Fig. 4. (A) Western blotting analysis of D54 and U251 control cells; (B) D54 and (C) U251 cells treated with 10–100 nM of TPT for 24–72 h.

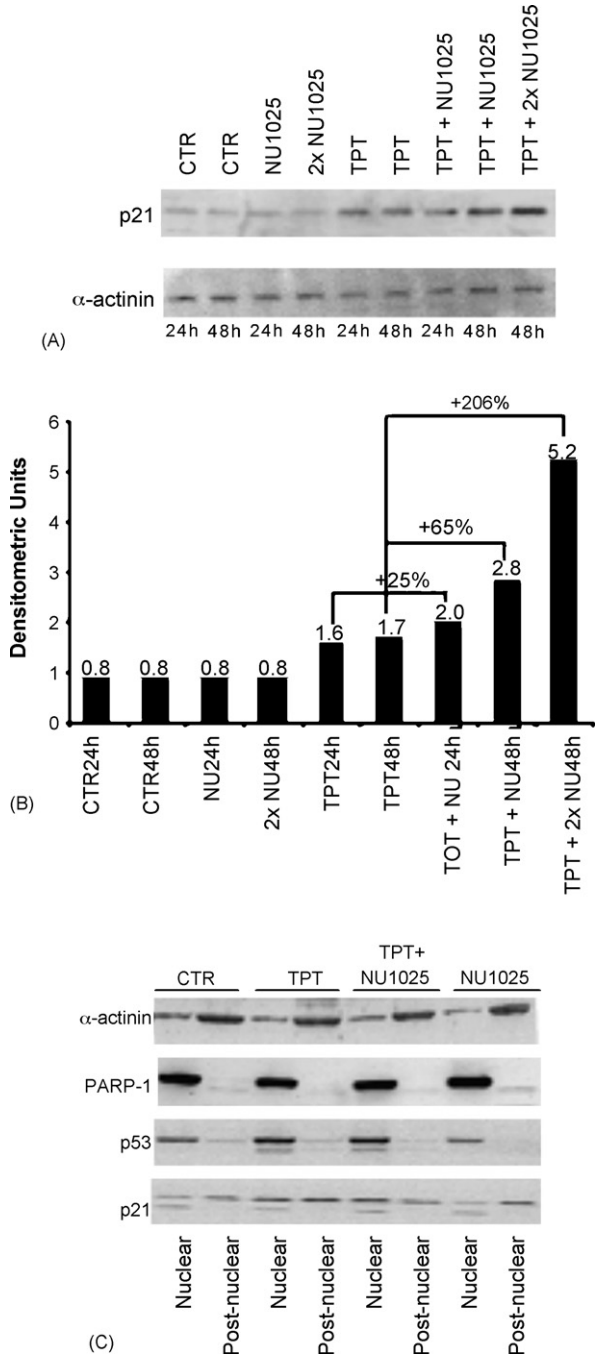

Fig. 5. (A) Western blotting analysis and (B) densitometric scanning of D54 cells control and 10 nM TPT treated ± a single or a double dose of 10 μM NU1025 with 24 h interval. The densitometric units determined for the immunoreactive bands are reported. (C) Western blotting analysis of nuclear and post-nuclear fractions of D54 cells 48 h treated with 10 nM TPT ± 10 μM NU1025.

Furthermore, endogenous levels of PARP-1, TOPO I, p53 and p21 in both D54 and U251 cells were evaluated by Western blotting. Fig. 4A shows a different p53 content in D54 and U251 cells, whereas the amount of TOPO I and PARP-1, as well as of p21, appeared to be the same in both cell lines.

Treatment with 10 or 100 nM TPT increased p53 and p21 levels in D54, starting at 24 h (Fig. 4B). We found that in D54 cells the p53 and p21 levels were increased by 24 or 48 h after treatment with TPT 10 or 100 nM. As expected, p53 over-expression preceded that of its target protein p21 (Fig. 4B). Conversely, the level of the inactive mutant form of p53 present in U251 cells did not change at any of the TPT treatments and no stimulation of p21 expression occurred (Fig. 4C).

Next, we investigated the effect of 10 nM TPT and 10 μM NU1025 combined treatment on p53 transcriptional activity by looking at changes in p21 expression in D54 cells. In Fig. 5A is shown that NU1025 alone, given as a single or double dose with 24 h interval (2×), was unable to increase p21 protein levels, while p21 expression was stimulated in the combined treatment. Such an effect was more pronounced when cells received a second dose of NU1025. The increase of p21 level was quantified in terms of densitometric units (DU) of the immunoreactive bands (Fig. 5B): after 24 and 48 h, a single dose of NU1025 in combination with TPT determined a 25% and 65% increase of p21 level compared to TPT alone. Moreover, a double dose of NU1025 further increased p21 level up to 206%.

Such evidences were related to the stabilisation of the nuclear localisation of p53 and p21. Fig. 5C shows the result of a Western blotting analysis of nuclear and post-nuclear fractions of D54 cells. The presence of an immunoreactive band for PARP-1 only in the nuclear fraction and of an immunoreactive band for α-actinin mainly in the post-nuclear fraction was taken as a proof of an efficient separation. TPT increased p53 level in the nuclear fraction and p21 level both in the nuclear and post-nuclear fractions. Moreover, the TPT-NU1025 combined treatment induced a specific increase of p21 in the nuclear fraction only.

Thereafter, the induction of apoptosis triggered by co-treatment with 10 nM TPT and 10 μM NU1025 in D54 and U251 cells was evaluated. Fig. 6A shows the result of TUNEL assay, that demonstrated an apoptosis increase in U251 (60% of positive cells) after combined treatment compared to TPT alone (40% of positive cells). This result was confirmed by Western blot analysis that showed the presence of the 89 kDa apoptotic fragment of PARP-1 deriving from the activation of the nuclear caspases (Fig. 6B).

Conversely, apoptosis was not detectable in D54 cells: however, cells accumulated at the G_2/M boundary and appeared larger in size due to hyperploidy (data not shown). Therefore, we conclude that cytostasis was the prominent effect induced by the combined treatment.

4. Discussion

Inhibition of PARP activity can be considered a new tool in the critical challenge to increase the sensitivity of cancer cells to chemotherapy. Wharton et al. [20] suggested that the high basal level of PARP and PAR in glioblastomas could play a role in the resistance to different cytotoxic agents and that the use of PARP inhibitors could be useful to revert such resistance. In this paper, we present evidences that the PARP inhibitor NU1025 at non-cytotoxic dose, potentiates the TPT chemotherapeutic action in glioblastoma cells. Interestingly, our evidences suggest that the PARP inhibitor function as adjuvant of the TOPO I poison is more pronounced in $D54^{p53wt}$ than in $U251^{p53mut}$ cells.

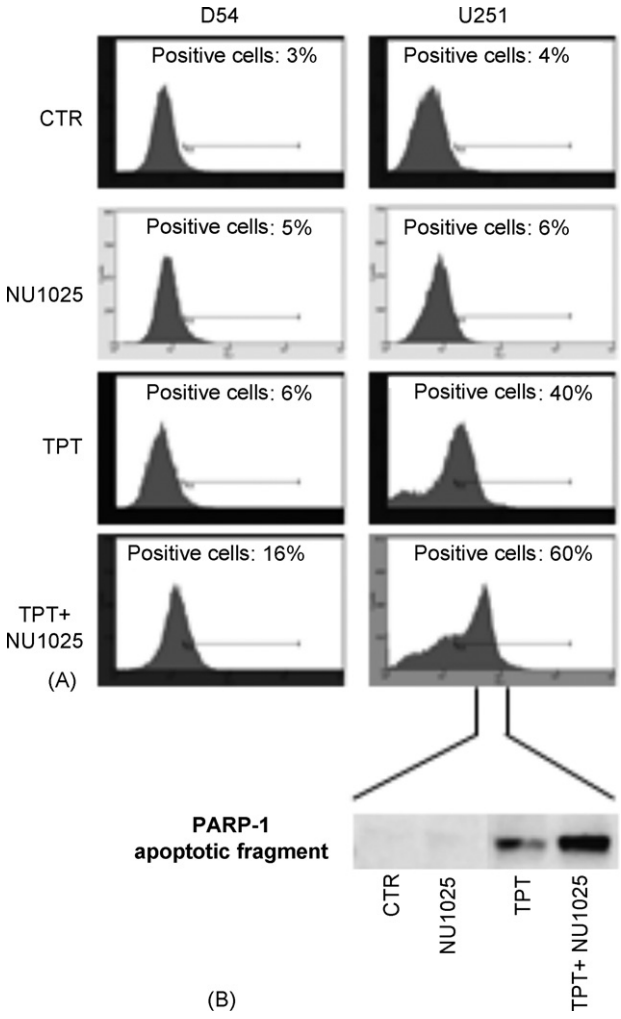

Fig. 6. (A) TUNEL assay of D54 and U251 cells 72 h treated with 10 nM TPT ± 10 μM NU1025. Data refer to one of three experiments giving similar results. (B) Western blotting analysis of PARP-1 apoptotic proteolysis in U251 cells 72 h treated with 10 nM TPT ± 10 μM NU1025.

Moreover, we found that NU1025 increased the G_2/M block of the cell cycle induced by TPT, in both $D54^{p53wt}$ and $U251^{p53mut}$ cell lines.

Thus, our findings agree with the observation that p53 status regulates the sensitivity of glioblastoma cells to TOPO I inhibitors [21,22]. Indeed, we observed that p53 is important in the ultimate fate of TPT-treated cells: very few p53 proficient D54 cells underwent apoptosis although many of them underwent a prolonged G_2/M arrest. On the other hand, in p53-mutated U251 cells the onset of the apoptosis was clearly evident starting from 48 h, driven by the caspase-dependent PARP-1 proteolysis. Interestingly, NU1025 addition determined an increment of both the G_2/M arrested D54 cells and of the U251 apoptotic cells.

While the role of PARP inhibitors as adjuvant of alkylating agents is quite understood [23,24], the mechanism that underlies their potentiation of TOPO I poisons still needs investigation.

We got evidences of the involvement of the PARP(s) activity in response to TPT-dependent DNA damage. We found a PARP(s) stimulation 24 h after TPT treatment, suggesting a recognition of the DNA damage deriving from the formation of the TPT/TOPO I/DNA abortive complex. In this contest, Smith et al. [25] suggested that PARPs inhibitors potentiate TOPO I poisons-mediated cytotoxicity without affecting TOPO I activity, by increasing the persistence of DNA strand breaks.

Moreover, a cross-talk between PARP-1 and TOPO I has been reported also by others. Malanga and Althaus [26] showed that auto-modified PARP-1 and PARP-2 can remove stalled TOPO I from DNA, resolving such kind of DNA damage. Yung et al. [27] referred of a PARP-1/TOPO I interaction regulated by TOPO I poly(ADP-ribosyl)ation. Park and Chen [28] demonstrated that PARP-1 facilitates the religation activity of TOPO I either through protein–protein interaction or by poly(ADP-ribosyl)ation of TOPO I. We found that in glioblastoma cells the PARP-1 auto-modification is the likely mechanism signalling DNA damage induced by TOPO I inhibitors.

PARP-1 and p53 modulation can be considered a promising therapeutic strategy for the involvement of both proteins in the induction/restoration of the apoptotic program of cell death. p53 is considered the major genome guardian protein that in response to DNA damage mediates cell cycle arrest or induces apoptosis, thereby suppressing malignant transformation [29].

The effect of p53 abrogation in the regulation of apoptosis has been reported in glioma cells in response to the alkylating agent temozolomide [30]. Our results point to a similar effect of both p53 and PARP-1 in cell death induced by TOPO I inhibitors.

Biochemical and genetic studies suggest a possible interaction of PARP-1 and p53 in mammalian cells. PARP-1 can bind to specific domains of p53 protein and modify p53 activity by poly(ADP-ribosyl)ation [31,13]. In *parp-1*$^{-/-}$ mice the induction of p53 in response to DNA damage is altered [32]. *In vivo* dominant negative inhibition of PARP activity, or siRNA down-regulation of PARP-1 resulted in a higher and prolonged p53 activation [33,34].

Our findings are consistent with these evidences, showing the stabilization of the p53 transcriptional activity as a consequence of the abrogation of PARP-1 activity. Moreover, we show for the first time that PARP-1 inhibitors further enhance the p21 over-expression induced by TOPO I inhibition. This evidence, together with the prolonged cytostastic effect at G_2/M boundary of their cell cycle, suggests a synergic action of PARP-1 and p53 as check-point proteins in the choice between cell death or survival in D54 cells.

Our results contribute to the understanding of the DNA-damaging process deriving from TOPO I inhibition and involving PARPs and p53. In this regard, it has been recently reported [35] that PARP-1 antagonizes TOPO I-dependent homologous recombination stimulated by p53. More studies are needed to clarify the cross-talk among these proteins and to identify the PARPs target proteins that represent the intermediate players in the signalling of the DNA damage deriving from TOPO I inhibition.

Nevertheless, our findings confirm that the combination of PARP-1 and TOPO I inhibitors could be an effective strategy to ameliorate the effects of chemotherapy on glioblastoma cells apart from the p53 status of the tumours.

Acknowledgements

This work was supported by AIRC 2002 and PRIN 2004 funding.

References

[1] Shah MA, Schartz GK. Cell-cycle mediated drug resistance: an emerging concept in cancer therapy. Clin Cancer Res 2001;7:2168–81.
[2] Cobbs CS, Whisenhunt TR, Weseman DR, Harkins LE, Van Meir EG, Samanta M. Inactivation of wild-type p53 protein function by reactive oxygen and nitrogen species in malignant glioma cells. Cancer Res 2003;63(24):8670–3.
[3] Wang Y, Zhu S, Cloughesy TF, Liau LM, Mischel PS. p53 disruption profoundly alters the response of human glioblastoma cell to DNA topoisomerase inhibition. Oncogene 2004;23(6):1283–90.
[4] Wang JC. Cellular role of DNA topoisomerases: a molecular perspective. Nat Rev Mol Cell Biol 2002;3:430–40.
[5] Garcia-Carbonero R, Supka JG. Current perspectives on the clinical experience, pharmacology, and continued development of the camptothecins. Clin Cancer Res 2002;8:641–61.
[6] Blaney SM, Cole DE, Balis FM, Godwin K, Poplack DG. Plasma and cerebrospinal fluid pharmokinetic study of topotecan in non human primates. Cancer Res 1993;53:725–7.
[7] Friedman HS, Houghton PJ, Schold SC, Keir S, Bigner DD. Activity of 9-dimethylaminoethyl-10-hydroxycamptothecin against pediatric and adult central nervous system tumor xenografts. Cancer Chemother Pharmacol 1994;34:171–4.
[8] Delaney CA, Wang LZ, Kyle S, White AW, Calvert AH, Curtin NJ, et al. Potentiation of temozolomide and topotecan growth inhibition and cytotoxicity by novel poly(adenosine diphosphoribose) polymerase inhibitors in a panel of human tumor cell lines. Clin Cancer Res 2000;6(7): 2860–7.
[9] Bürkle A. Physiology and patho-physiology of poly(ADP-ribosyl)ation. BioEssays 2001;23:795–806.
[10] Rolli V, Ruf A, Augustin A, Schulz GE, Menissier de Murcia J, de Murcia G. Poly(ADP-ribose)polymerase structure and function. In: de Murcia G, Shall S, editors. DNA damage and stress signalling to cell death. Poly ADP-ribosylation reactions. Oxford University Press; 2000. p. 35–57.
[11] Pleschke JM, Kleczkowska HE, Strohm M, Althaus FR. Poly(ADP-ribose) binds to specific domains in DNA damage checkpoint proteins. J Biol Chem 2000;275:40974–80.
[12] Mendoza-Alvarez H, Alvarez-Gonzalez R. Regulation of p53 sequence-specific DNA-binding by covalent poly(ADP-ribosyl)ation. J Biol Chem 2001;276(39):36425–30.
[13] Malanga M, Pleschke JM, Kleczkowska HE, Althaus FR. Poly(ADP-ribose) binds to specific domains of p53 and alters its DNA binding functions. J Biol Chem 1998;273(19):11839–43.
[14] Ferro AM, Olivera BM. Poly(ADP-ribosylation) of DNA topoisomerase I from calf thymus. J Biol Chem 1984;259(1):547–54.
[15] Scovassi AI, Poirier GG. Poly(ADP-ribosyl)ation and apoptosis. Mol Cell Biochem 1999;199:125–37.
[16] Beneke S, Diefenbach J, Burkle A. Poly(ADP-ribosyl)ation inhibitors: promising drug candidates for a wide variety of pathophysiologic conditions. Int J Cancer 2004;111:813–8.
[17] Bowman KJ, Newell DR, Calvert AH, Curtin NJ. Differential effects of the poly (ADP-ribose) polymerase (PARP) inhibitor NU1025 on Topoisomerase I and II inhibitor cytotoxicity in L1210 cells in vitro. Br J Cancer 2001;84(1):106–12.
[18] Chou TC, Talalay P. Quantitative analysis of dose–effect relationships: the combined effects of multiple drugs or enzyme inhibitors. Adv Enzyme Regul 1984;22:27–55.
[19] Di Meglio S, Tramontano F, Cimmino G, Jones R, Quesada P. Dual role for poly(ADP-ribose)polymerase-1 and -2 and poly(ADP-ribose)glycohydrolase as DNA-repair and pro-apoptotic factors in rat germinal cells exposed to nitric oxide donors. BBA Mol Cell Res 2004;1692(1):35–44.
[20] Wharton SB, McNelis U, Bell HS, Whittle IR. Expression of poly(ADP-ribose) polymerase and distribution of poly(ADP-ribosyl)ation in glioblastoma and in a glioma multicellular tumour spheroid model. Neuropath Appl Neurobiol 2000;26:528–53.
[21] Gobert C, Skladanowski A, Larsen AK. The interaction between p53 and DNA topoisomerase I is regulated differently in cells with wild-type and mutant p53. Proc Natl Acad Sci USA 1999;96(18):10355–6.
[22] Tomicic MT, Christmann M, Kaina B. Topotecan-triggered degradation of Topoisomerase I is p53 dependent and impacts cell survival. Cancer Res 2005;65(19):8920–6.
[23] Tentori L, Portarena I, Torino F, Scerrati M, Navarra P, Graziani G. Poly(ADP-ribose) polymerase inhibitor increases growth inhibition and reduces G(2)/M cell accumulation induced by temozolomide in malignant glioma cells. Glia 2002;40(1):44–54.
[24] Tentori L, Graziani G. Chemopotentiation of PARP inhibitors in cancer therapy. Pharmacol Res 2005;52:25–33.
[25] Smith LM, Willmore E, Austin CA, Curtin N. The novel poly(ADP-ribose)polymerase inhibitor AG14361, sensitizes cells to Topoisomerase I poisons by increasing the persistence of DNA strand breaks. Clin Cancer Res 2005;11(23):8449–57.
[26] Malanga M, Althaus FR. Poly(ADPribose) reactivates stalled DNA topoisomerase I and induces DNA strand breaks resealing. J Biol Chem 2004;279(7):5244–8.
[27] Yung TMC, Sato S, Satoh MS. Poly(ADP-ribosyl)ation as a DNA damage-induced post-translational modification regulating Poly(ADPR) polymerase-1 Topoisomerase I interaction. J Biol Chem 2004;38(17): 39686–96.
[28] Park SY, Cheng YC. Poly(ADP-ribose) polymerase could facilitate the religation of topoisomerase I-linked DNA inhibited by camptothecin. Cancer Res 2005;65(9):3894–902.
[29] Levine AJ. p53, the cellular gatekeeper for growth and division. Cell 1997;88(3):323–31.
[30] Hirose Y, Berger MS, Pieper RO. p53 effects both the duration of G2/M arrest and the fate of temozolomide-treated human glioblastoma cells. Cancer Res 2001;61(5):1957–63.
[31] Wesierska-Gadek J, Wojciechowski J, Schmid G. Central and carboxy-terminal regions of human p53 protein are essential for interaction and complex formation with PARP-1. J Cell Biochem 2003;89(2):220–32.
[32] Agarwal ML, Agarwal A, Taylor WR, Wang ZQ, Wagner EF, Stark GR. Defective induction but normal activation and function of p53 in mouse cells lacking poly-ADP-ribose polymerase. Oncogene 1997;15(9):1035–41.
[33] Beneke R, Geisen C, Zevnik B, Bauch T, Muller WU, Kupper JH, et al. DNA excision repair and DNA damage-induced apoptosis are linked to poly(ADP-ribosyl)ation but have different requirements for p53. Mol Cell Biol 2000;20(18):6695–703.
[34] Simbulan-Rosenthal CM, Rosenthal DS, Ding R, Bhatia K, Smulson ME. Prolongation of the p53 response to DNA strand breaks in cells depleted of PARP by antisense RNA expression. Biochem Biophys Res Commun 1998;253(3):864–8.
[35] Bauman C, Boehden GS, Burkle A, Wiesmuller L. Poly(ADP-ribose) polymerase-1 (PARP-1) antagonizes topoisomerase I-dependent recombination stimulation by p53. Nucleic Acids Res 2006;34(3):1036–49.